

Article

Selective Extraction and Determination of Hydrocortisone and Dexamethasone in Skincare Cosmetics: Analytical Interpretation Using Statistical Physics Formalism

Fatma Aouaini ^{1,*} , Nadia Bouaziz ², Ahlem Cherif ³, Haifa A. Alyousef ¹ and Abdelmottaleb Ben Lamine ²

¹ Department of Physics, College of Science, Princess Nourah Bint Abdulrahman University, Riyadh 11564, Saudi Arabia; halyousef@pnu.edu.sa

² Laboratory of Quantum and Statistical Physics, LR18ES18, Faculty of Sciences of Monastir, Monastir University, Monastir 5000, Tunisia; bouaziznadia56@yahoo.com (N.B.); aben_lamin@yahoo.fr (A.B.L.)

³ Department of Physics, College of Science, Jouf University, Sakaka P.O. Box 2014, Saudi Arabia; amnajima@ju.edu.sa

* Correspondence: fasaidi@pnu.edu.sa

Abstract: Molecularly imprinted polymers (MIPs), as magnetic extraction adsorbents, are used for the selective, rapid determination and extraction of dexamethasone and hydrocortisone in skincare products. Therefore, in this paper, magnetic molecularly imprinted polymers (MMIPs) and magnetic non-molecularly imprinted polymers (MNIPs) were utilized as adsorbents to describe the adsorption phenomena of dexamethasone and hydrocortisone. This interpretation, based on a statistical physics theory, applies the multilayer model with saturation to comprehend the adsorption of the drugs. Results obtained via numerical simulation revealed that dexamethasone and hydrocortisone adsorption happens via a non-parallel orientation on the surfaces of MMIPs and MNIPs, and they also showed that the adsorption amount of the MMIPs for the template molecule was notably greater than that of the MNIPs at the same initial concentration. The adsorption energy values retrieved from the data analysis ranged between 7.65 and 15.77 kJ/mol, indicating that the extraction and determination of dexamethasone and hydrocortisone is a physisorption process. Moreover, the distribution of a site's energy was calculated to confirm the physical nature of the interactions between adsorbate/adsorbent and the heterogeneity of the surfaces of the MMIPs and MNIPs. Finally, the thermodynamic interpretation confirmed the exothermicity and spontaneous nature of the adsorption of these drugs on the tested adsorbents.

Keywords: cosmetic samples; dexamethasone; hydrocortisone; MIPs; statistical physics



Citation: Aouaini, F.; Bouaziz, N.; Cherif, A.; Alyousef, H.A.; Lamine, A.B. Selective Extraction and Determination of Hydrocortisone and Dexamethasone in Skincare Cosmetics: Analytical Interpretation Using Statistical Physics Formalism. *Appl. Sci.* **2024**, *14*, 2077. <https://doi.org/10.3390/app14052077>

Academic Editor: Burkhard Poeggeler

Received: 22 September 2023

Revised: 23 January 2024

Accepted: 29 January 2024

Published: 1 March 2024



Copyright: © 2024 by the authors. Licensee MDPI, Basel, Switzerland. This article is an open access article distributed under the terms and conditions of the Creative Commons Attribution (CC BY) license (<https://creativecommons.org/licenses/by/4.0/>).

1. Introduction

Corticosteroids are known to be extremely efficient drugs and are broadly employed for the treatment of inflammatory skin diseases like eczema, dermatoses, and psoriasis [1–3] to tentatively alleviate their symptoms [4,5].

Dexamethasone and hydrocortisone, as types of corticosteroids, are mostly used in the form of ointments, gels, and creams, with varying potentiality and efficiency for topical use [6,7]. For this reason, certain producers illegally put dexamethasone and hydrocortisone in cosmetics to enhance the effects of their commercially accessible products. The application of cosmetics provides many benefits, including preventing human skin from aging, increasing elasticity, and eliminating wrinkles. In a majority of cases, cosmetics are utilized daily by teenagers, men, and women, and this prolongs the exposure of skin to cosmetics. Prolonged use of cosmetics contaminated by dexamethasone or hydrocortisone can cause many grave adverse effects to arise, such as cutaneous reactivity, skin atrophy, some systematic side effects, diabetes mellitus, and hypertension [7,8].

According to EU Cosmetics Regulations, corticosteroids like dexamethasone and hydrocortisone have been prohibited in the creation of cosmetic products [9]. Thus, there is

an obligation to research and produce efficient and rapid technology for screening dexamethasone or hydrocortisone in cosmetics. Currently, there are many conventional methods for detecting these hormones in cosmetics, such as ionic liquid micro extraction [10], solid phase extraction (SPE) [11,12], and liquid phase extraction [13–15]. Unfortunately, these technologies are often time-consuming, difficult to use, and need great quantities of reagents and solvents. Thus, choosing a suitable sample preparation technique is key for the effective examination of complex samples.

MIPs are made using molecular imprinting methods and are designed to selectively acknowledge target molecules [16]. MIPs are simple to make and provide better selectivity for substrates compared with conventional separation technologies. However, when MIPs are utilized for the extraction of absorbed target molecules, there is frequently a loss of certain substances. In order to minimize this disadvantage, magnetic molecular imprinted polymers (MMIPs) are seeing a gradual increase in utilization in separation applications and substance treatment [17,18]. MMIPs are defined by more precise selectivity for guest molecules and unique magnetic response characteristics [19,20]. Liu et al. tested the ability MMIPs and MNIPs to separate dexamethasone and hydrocortisone from cosmetic products [21]; adsorption proved to be successful for the extraction of the target molecules (hydrocortisone and dexamethasone) from the cosmetics samples due to their great extraction efficiency, versatility, and simple operation (in terms of the characteristics of the adsorbents). Hydrocortisone and dexamethasone adsorption isotherms were used to analyze and understand the adsorption process and to describe the behavior of the adsorption amount and adsorbent affinity. A statistical physics treatment based on analytical models was adopted to theoretically describe the adsorption isotherms, and this reflected a saturated adsorption process at elevated concentrations.

The aim of this article is to comprehend the adsorption phenomena of hydrocortisone and dexamethasone on magnetic molecularly imprinted polymer (MMIP) and magnetic non-molecularly imprinted polymer (MNIP) adsorbents through the application of statistical physics formalism, and to carry out a corresponding investigation of the physicochemical parameters that present a clear physical correlation with the adsorption phenomena. This work gives advanced theoretical results on the adsorption of cosmetic products using molecularly imprinted polymers.

2. Experimental

The method used for the preparation and characterization of the dual-template MNIPs/MMIPs was that reported by Min Liu et al. [21]. The experimental procedure was carried out with both MNIPs and MMIPs for comparison. A precise quantity of the MNIP and MMIP adsorbents was weighed out and added to a concentration of a dexamethasone and hydrocortisone solution in a conical flask. The MMIP and MNIP adsorbents which attained adsorption equilibrium were separated from the aforementioned solution using an external magnetic field.

The experimental data of the MNIPs and MMIPs with dexamethasone and hydrocortisone were measured as described in reference [21]. Using UV–Vis measurements, the adsorption capacities of the dual-template MNIPs/MMIPs were determined utilizing the following equation:

$$Q = (C_0 - C_e) \times V/W \quad (1)$$

where Q is the dexamethasone or hydrocortisone quantity related to the MNIPs/MMIPs at equilibrium, W defines the quality of the MNIPs/MMIPs, V is the solution volume, C_e is the concentration, at equilibrium, of free dexamethasone or hydrocortisone in the solution, and C_0 is the initial concentration of dexamethasone or hydrocortisone.

These data were then used to trace the adsorption isotherms of the MNIPs and MMIPs as functions of the dexamethasone or hydrocortisone concentrations, as presented in Figure 1.

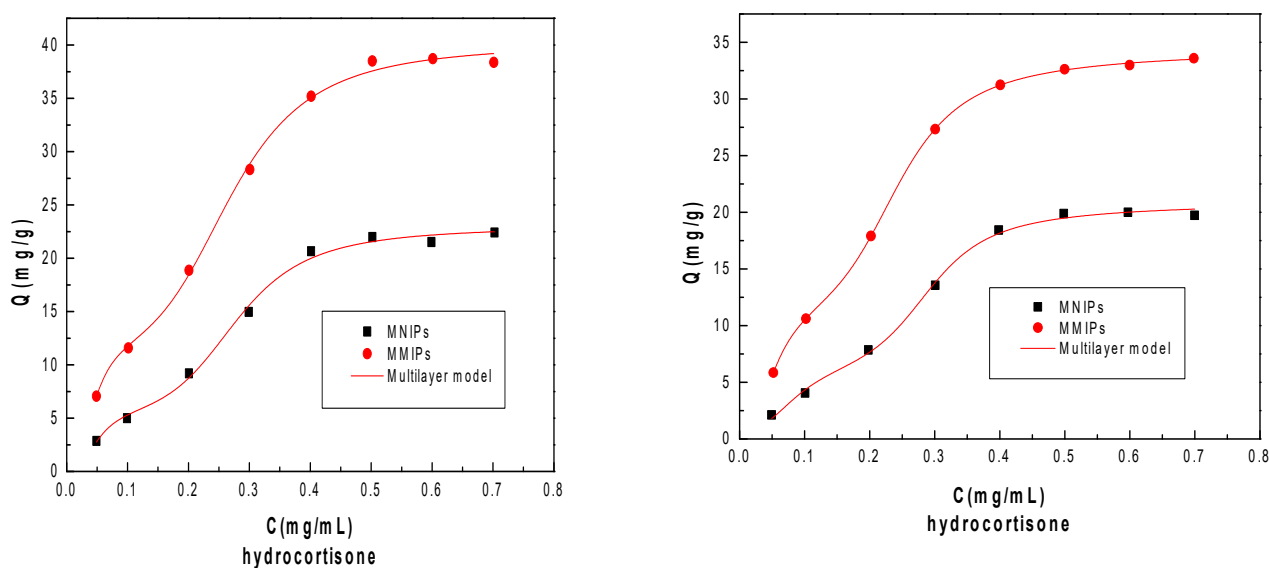


Figure 1. Adsorption isotherms of hydrocortisone and dexamethasone on dual-template MMIPs and MNIPs. Experimental data fitted using the multilayer statistical model M3 (continuous lines).

3. Description of Adsorption Isotherms and Modeling Investigation

The experimental adsorption isotherms of the dexamethasone and hydrocortisone on the MNIP and MMIP adsorbents are presented in Figure 1. As can be noted, the isotherms of adsorption are monotonic regarding the equilibrium concentration. At elevated dexamethasone or hydrocortisone equilibrium concentrations, the adsorption amounts for the MNIP and MMIP adsorbents tended to plateau, coinciding with the saturation of the adsorbents. The saturation plateau is correlated to the complete filling of the accessible adsorption sites of the dual-template MNIPs/MMIPs by the dexamethasone and hydrocortisone solutions, leading to a number of dexamethasone or hydrocortisone adsorption layers. In addition, the various adsorption amounts are helpful for designating the adsorbent affinity. Particularly, the MMIP adsorbent indicated greater selectivity towards the dexamethasone solution.

In addition to experimental proof, which does not describe the adsorption process, an efficient modeling interpretation was necessary to further our understanding, and this will be depicted in the upcoming section. To this aim, three physical models were established based on statistical physics and tested on the experimental data. The analysis of the adsorption phenomena was carried out by utilizing the grand canonical ensemble to take account of the particle number variation by inserting a variable chemical potential in the adsorption phenomena [22–24].

3.1. Model 1: Single Layer (M1)

This model presumed that dexamethasone and hydrocortisone adsorption takes place through the creation of a single adsorbed layer with equal energy (Figure 2). In this case, each receptor site present in the adsorbent captures a variable number of molecules, characterized through the parameter n . The adsorbed amount versus the equilibrium concentration is expressed as follows [25]:

$$Q_a = \frac{nD_m}{1 + \left(\frac{C_{1/2}}{C}\right)^n} \quad (2)$$

where $C_{1/2}$ defines the half-saturation concentration and D_m defines the receptor site's density of adsorbents.



Figure 2. Schematic illustration of the distribution of the molecules adsorbed onto a solid according to the monolayer model with single energy.

3.2. Model 2: Double Layer (M2)

For this model, dexamethasone and hydrocortisone adsorption can take place through the creation of two adsorbed layers (Figure 3). It is supposed that the molecules are adsorbed with two varying adsorption energies. The adsorbed amount versus the equilibrium concentration is expressed as follows [26]:

$$Q_a = nD_m \frac{\left(\frac{C}{C_1}\right)^n + 2\left(\frac{C}{C_2}\right)^{2n}}{1 + \left(\frac{C}{C_1}\right)^n + \left(\frac{C}{C_2}\right)^{2n}} \tag{3}$$

where C_1 and C_2 are, respectively, the half-saturation concentrations of the first and second layers.

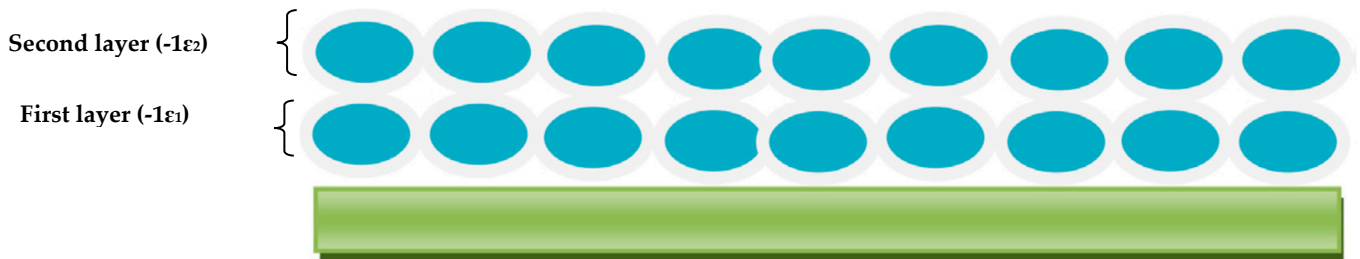


Figure 3. Schematic illustration of the distribution of the molecules adsorbed onto a solid according to the double-layer model with two energies.

3.3. Model 3: Multilayer (M3)

The third analytical model assumes that dexamethasone and hydrocortisone molecules are adsorbed through a multi-layer mechanism with saturation (Figure 4). Two adsorption energies are present in this case, and these are related to adsorbate–adsorbent and adsorbate–adsorbate interactions. Generally, the total number of adsorbed layers is defined as $N_c = 1 + N_2$. The expression of the multilayer model is given as follows [27,28]:

$$Q_a = n.D_m \cdot \frac{\frac{-2\left(\frac{C}{C_1}\right)^{2n}}{\left(1-\left(\frac{C}{C_1}\right)^n\right)} + \frac{\left(\frac{C}{C_1}\right)^n \left(1-\left(\frac{C}{C_1}\right)^{2n}\right)}{\left(1-\left(\frac{C}{C_1}\right)^n\right)^2} + 2 \frac{\left(\frac{C}{C_1}\right)^n \left(\frac{C}{C_2}\right)^n \left(1-\left(\frac{C}{C_2}\right)^{nN_2}\right)}{\left(1-\left(\frac{C}{C_2}\right)^n\right)} - \frac{\left(\frac{C}{C_1}\right)^n \left(\frac{C}{C_2}\right)^n \left(\frac{C}{C_2}\right)^{nN_2} N_2 \left(1-\left(\frac{C}{C_2}\right)^n\right)}{\left(1-\left(\frac{C}{C_2}\right)^n\right)} + \frac{\left(\frac{C}{C_1}\right)^n \left(\frac{C}{C_2}\right)^{2n} \left(1-\left(\frac{C}{C_2}\right)^{nN_2}\right)}{\left(1-\left(\frac{C}{C_2}\right)^n\right)^2}}{\frac{\left(1-\left(\frac{C}{C_1}\right)^{2n}\right)}{\left(1-\left(\frac{C}{C_1}\right)^n\right)} + \frac{\left(\frac{C}{C_1}\right)^n \left(\frac{C}{C_2}\right)^n \left(1-\left(\frac{C}{C_2}\right)^{nN_2}\right)}{\left(1-\left(\frac{C}{C_2}\right)^n\right)}} \tag{4}$$

where C_1 and C_2 are, respectively, the half-saturation concentrations of the first and other created layers (N_2 layers).

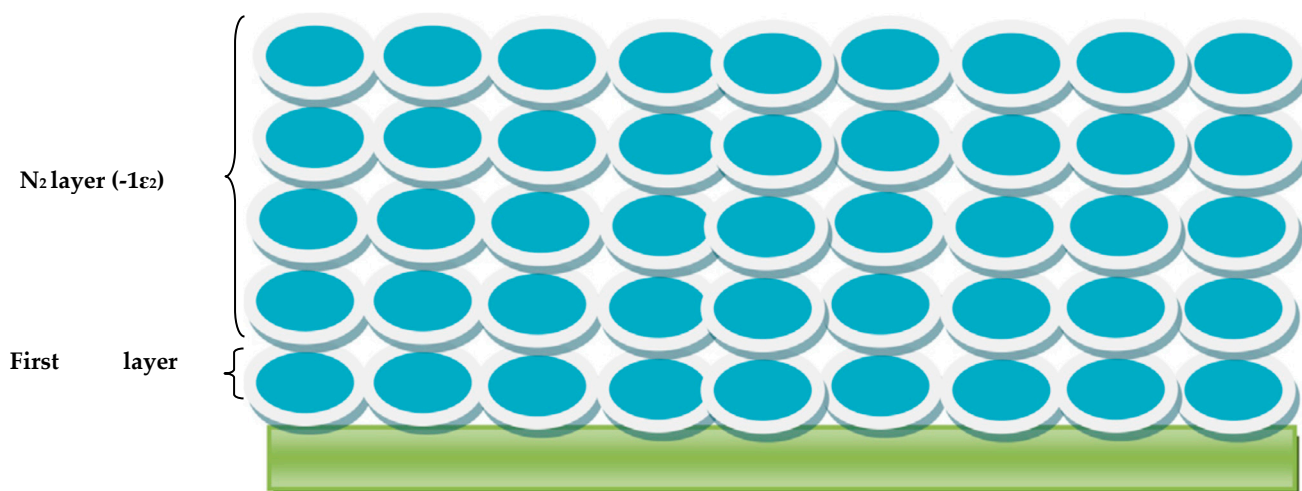


Figure 4. Schematic illustration of the distribution of the molecules adsorbed onto a solid according to the multilayer model with saturation.

3.4. Fitting Results and Discussion

The experimental data depicted in Figure 1 were adjusted using three analytical models. In general, numerical results show that the parameters of monolayer and double-layer models are not theoretically consistent enough to supply a correct understanding of the dexamethasone and hydrocortisone adsorption processes in dual-template MNIPs and MMIPs. As an example, the adsorption capacity values determined using numerical simulations for the dexamethasone and hydrocortisone solutions were very elevated and inconsistent with the experimental results. These models are not appropriate for the study of the adsorption mechanisms of dexamethasone and hydrocortisone solutions. The parameters of the multilayer model were more accurate with the correlation coefficient R^2 near unity, and the residual root mean square error (RMSE) values were close to zero (Table 1).

Table 1. Values of the adjustment coefficient R^2 and the residual root mean square error (RMSE) for the three proposed fitting models.

Adsorbate	Adsorbent	Coefficient of Determination R^2			RMSE		
		M1	M2	M3	M1	M2	M3
Hydrocortisone	MNIPs	0.869	0.977	0.999	0.716	0.107	0.03
	MMIPs	0.816	0.961	0.997	0.745	0.134	0.07
Dexamethasone	MNIPs	0.726	0.982	0.999	0.830	0.207	0.06
	MMIPs	0.803	0.911	0.998	0.862	0.311	0.04

The choice of the multilayer model can be further explained by the following reasons. Firstly, both MMIPs and MNIPs may exhibit a certain degree of surface roughness or nanoscale irregularities. These irregularities can create additional binding sites for dexamethasone and hydrocortisone molecules, thereby promoting multilayer adsorption [29]. Additionally, molecularly imprinted polymers (MIPs) are synthetic multifunctional materials characterized by a high affinity and specificity for target molecules [30–32], enabling the adsorption of multiple layers of these molecules onto the polymer's surface. These high-affinity interactions can lead to the formation of multiple layers as dexamethasone and hydrocortisone molecules compete for the available binding sites.

Therefore, the multilayer model is used in this article to describe dexamethasone and hydrocortisone adsorption on MNIPs and MMIPs. The adjusted parameters of the chosen model are summarized in Table 2. Figure 1 presents the fit of this model to all the experimental adsorption data and shows an excellent accordance.

Table 2. Values of adjustment parameters corresponding to the fitting of hydrocortisone and dexamethasone isotherms on dual-template MMIPs and MNIPs with the multilayer model (M3).

Adsorbate	Adsorbent	Parameter					
		n	D_m	N_c	Q_{sat} (mg/g)	C_1 (mg/mL)	C_2 (mg/mL)
Hydrocortisone	MNIPs	2.675	1.830	3.240	15.41	0.057	0.282
	MMIPs	3.184	3.422	2.101	22.83	0.049	0.242
Dexamethasone	MNIPs	2.738	2.084	3.321	18.70	0.050	0.281
	MMIPs	3.757	4.373	2.328	38.01	0.043	0.238

4. Physical Interpretation of Steric Parameters

4.1. Parameters n , D_m , and N_c

The steric parameter n contributes by providing descriptive details concerning the adsorption process of dexamethasone and hydrocortisone molecules on MNIPs and MMIPs adsorbents. For example, the adsorption orientation of the dexamethasone and hydrocortisone solutions on the surfaces of the MNIPs and MMIPs is explained using this parameter. Numerous works in the literature [33,34] have reported that three plausible manners arise for depicting the orientation of adsorption using the n values.

- **Possibility 1:** for the case of $n < 0.5$, the receptor sites of the MNIP and MMIP adsorbents capture a portion of the dexamethasone and hydrocortisone molecules (i.e., the molecules are shared by two or more receptor sites), implying a parallel adsorption orientation. Therefore, the adsorption is defined as a multi-interaction process.
- **Possibility 2:** for the case of $0.5 < n < 1$, a mixed adsorption orientation can be observed, i.e., the molecules are captured via non-parallel and parallel orientations simultaneously, with two proportions.
- **Possibility 3:** for the case of $n \geq 1$, the receptor sites capture one or more molecules, showing a non-parallel adsorption orientation. Consequently, this adsorption is defined as a multi-molecular process.

According to the numerical simulation results given in Table 2, the adsorption values of n are equal to 2.67 and 3.18 for hydrocortisone and are equal to 2.73 and 3.75 for dexamethasone on MNIP and MMIP adsorbents, respectively. These values are greater than 1, showing that the hydrocortisone and dexamethasone solutions are adsorbed in a non-parallel orientation through their interactions with the MNIP and MMIP adsorbents, which indicates that this adsorption is multi-molecular. For instance, the value of n for hydrocortisone adsorption on dual-template MMIPs is 2.65. This value, when examined using the equation $2.65 = 2 \times p + (1 - p) \times 3$, indicates that the number of hydrocortisone molecules adsorbed per site ranges between two and three. This equation can be used to calculate the exact proportions, where p represents the sites binding with two molecules and $(1 - p)$ represents the sites binding with three molecules. This calculation shows that $p = 0.35$, i.e., 35% of the MMIP sites adsorbed two molecules and 65% of the sites adsorbed three hydrocortisone molecules. A comparison among the two adsorption systems demonstrated that this parameter varies as follows: $n(\text{hydrocortisone/MNIPs}) < n(\text{hydrocortisone/MMIPs})$ and $n(\text{dexamethasone/MNIPs}) < n(\text{dexamethasone/MMIPs})$. This difference is attributed to the complementary shape, spatial distribution, size, and molecular interactions of the imprinting sites in the MMIP cavities [21,35].

Parameter D_m represents the effectually occupied density of the receptor sites per surface unit of the adsorbent. According to Table 2, it is apparent that the receptor site density of the MMIPs is higher than that of the MNIPs in the cases of dexamethasone and hydrocortisone solutions. This can be explained by the experimental results revealed in ref [21], which show that the surface polymerization preparation of dual-template MMIPs results in a larger specific surface area.

Parameter N_c is defined as the total number of the adsorbed layers of hydrocortisone/dexamethasone ($N_c = 1 + N_2$) during the adsorption process. According to the modeling results summarized in Table 2, it can be noted that the total number of created layers for the two systems ranged between 2.1 and 3.3. This finding indicates that the adsorption of dexamethasone and hydrocortisone is almost attained via the creation of approximately two or three adsorbate layers. It was concluded that the number of layers that formed during adsorption was the result of the low interaction energies that play a major role in the dexamethasone and hydrocortisone recognition process. Indeed, the decrease in the number of efficient sites accessible for the adsorption of the dexamethasone and hydrocortisone onto the MMIP/MNIP surfaces was relatively equivalent through a multilayer adsorption mechanism. This can be explained by ranking adsorbents by their adsorption amount, which can be linked to the propensity to create multi-layers that can counterbalance the incidences of details unfavorable for adsorption.

4.2. Parameter Q_{sat}

Parameter Q_{sat} is the adsorption amount at saturation, whose expression is directly determined by the multilayer model when the hydrocortisone or dexamethasone concentration at equilibrium tends to infinity. This factor plays a pertinent role in showing the affinity of hydrocortisone/dexamethasone molecules towards the surfaces of MNIPs and MMIPs.

Adsorption capacity at saturation depends on the parameters n , D_m , and N_c through the following relation [36,37]:

$$Q_{sat} = n \times D_m \times N_c \quad (5)$$

The maximum adsorption capacities of hydrocortisone are 15.41 and 22.83 mg/g on dual-template MNIPs and MMIPs, respectively, while the adsorption amounts of dexamethasone at saturation are 18.7 and 38.01 mg/g, respectively, on MNIP and MMIP adsorbents (Table 2). It is obvious that the adsorption capacity of MMIPs is much higher than that of MNIPs at the same concentration of hydrocortisone and dexamethasone. This indicates that MMIPs show much better affinity towards dexamethasone or hydrocortisone, and that they preserve the spatial cavities of the template well. Furthermore, this difference is due to the imprinting effect of each adsorbent. Consequently, dexamethasone and hydrocortisone can undergo adsorption onto various sites of the MMIPs. This theoretical result is in agreement with the experimental data, which revealed that the MMIPs possessed a more elevated initial adsorption rate and a more elevated saturated adsorption capacity than the MNIPs [21].

5. Analysis of the Adsorption Energy

Adsorption energy is a significant parameter for studying adsorption and defining the types of interactions between adsorbate and adsorbent. Using the two half-saturation concentrations C_1 and C_2 , the estimation of the two adsorption energies, ΔE_1 and ΔE_2 , is possible by means of an analytical expression derived from statistical physics theory. In particular, ΔE_1 is associated with interactions between dexamethasone/hydrocortisone molecules and MMIP/MNIP surfaces on the first layer, whereas ΔE_2 represents interactions between the adsorbate particles on the second layer. The expressions of the adsorption energies are depicted by the following relations [38]:

$$\Delta E_1 = RT \ln \frac{C_s}{C_1} \quad (6)$$

$$\Delta E_2 = RT \ln \frac{C_s}{C_2} \quad (7)$$

where C_s is the solubility of the adsorbate, $R = 8.314472$ J/mol. K is the ideal gas constant, and T is the absolute temperature.

To investigate the adsorption phenomena, the energies ΔE_1 and ΔE_2 were determined for all systems at 25 °C. The calculated values of the adsorption energies summarized in

Table 3 are lower than 20 kJ/mol, thus proving the presence of physical forces, which can take the form of Van der Waals interactions or hydrogen bindings. The Van der Waals forces are usually of the order of 10 kJ mol⁻¹, and the hydrogen bindings generally show values below 30 kJ mol⁻¹ [25]. Therefore, the interactions between these two molecules can be estimated using the hydrogen binding interactions between hydroxyl group of the adsorbate molecule and the adsorbent receptor site. As expected, the second energy was lower than the first one because of the weaker interactions between the adsorbate and the adsorbate.

Table 3. Adsorption energy values of hydrocortisone and dexamethasone on dual-template MMIPs and MNIPs at 25 °C.

Adsorbate	Adsorbent	ΔE_1 (KJ/mol)	ΔE_2 (KJ/mol)
Hydrocortisone	MNIPs	11.617	7.656
	MMIPs	11.992	8.035
Dexamethasone	MNIPs	15.397	11.120
	MMIPs	15.770	11.531

6. Adsorption Energy Distribution (AED) Determination

The Polanyi potential theory [39–42] provides a means for deducing the distribution of adsorption energies at different sites. According to this theory, we rely on the adsorption energy (ϵ), which is related to the concentrations of the substances at half saturation, (C_1) and (C_2), to determine the site energy distribution using the following formula:

$$C = C_s e^{\frac{-\epsilon}{(RT)}} \quad (8)$$

where C_s is the solubility of the adsorbate, $R = 8.314472$ J/mol. K is the ideal gas constant, and T is the absolute temperature.

Furthermore, by integrating Equation (8) into the multilayer saturation model, equation (M3), the isotherm $Q_a = f(C)$ can be expressed as a function of ϵ . Upon differentiating the equation model with respect to ϵ , the site energy distribution $F(\epsilon)$ can be derived using Equation (9):

$$F(E) = \frac{\partial Q_a}{\partial E} \quad (9)$$

Figure 5 depicts the adsorption energy distributions (AEDs) for hydrocortisone and dexamethasone on the surfaces of the two adsorbent composites, the MNIPs and the MMIPs, in accordance with Equation (9). It is important to note that all the curves follow a similar normal distribution pattern but vary in the intensity of the energy associated with their respective peak values. In particular, the AED for the MMIP adsorbent's surface exhibits a broader range of adsorption energies compared with the AED for the MNIPs in the adsorption of hydrocortisone and dexamethasone. This indicates that binding sites with low adsorption energies become less accessible for the adsorption of the two adsorbates on the MNIP adsorbent. Indeed, the energy distribution plot shifts along the x -axis, revealing a singular peak that likely represents the average energy of the distributions of the two adsorbate molecules on the surfaces of both adsorbents (the MNIPs and MMIPs). Consequently, the MNIPs and MMIPs exhibit heterogeneous surfaces, with disparities in their maximum peak intensities attributed to variations in the functional activated groups of both the molecules and the adsorbent surfaces. Notably, the adsorption energy values are confined to 12 kJ/mol for hydrocortisone and 17 kJ/mol for dexamethasone adsorption. This observation solidifies the notion that this phenomenon primarily involves physisorption processes.

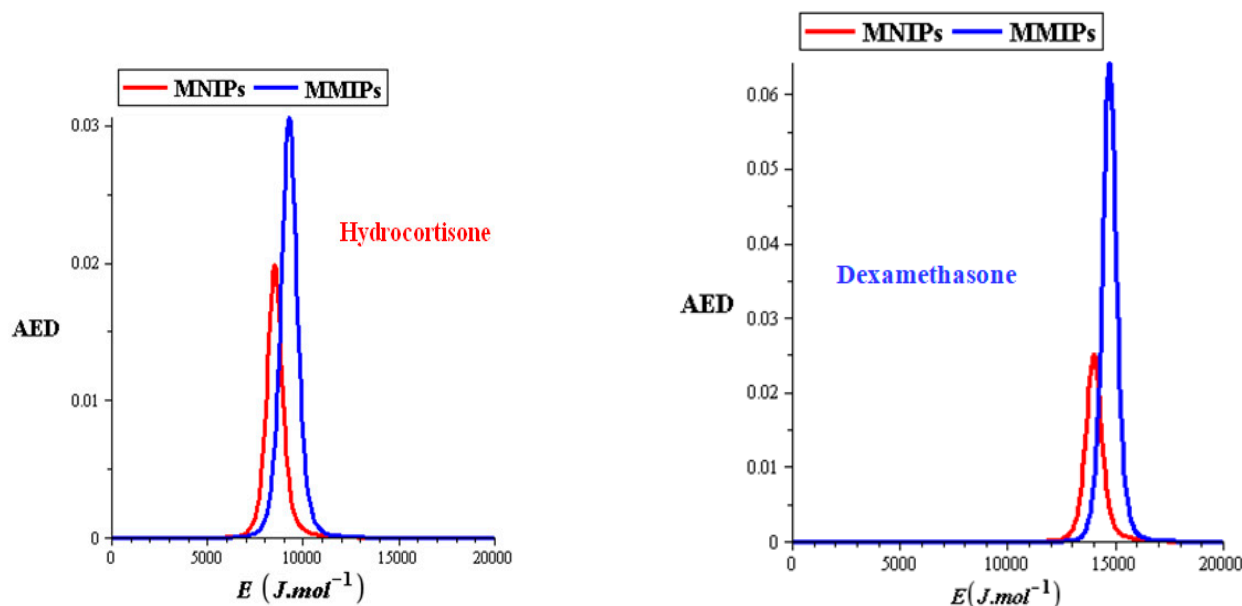


Figure 5. Adsorption energy distribution (AED) of hydrocortisone and dexamethasone on the surfaces of the two adsorbent composites (MNIPs and MMIPs).

7. Thermodynamic Interpretation

7.1. Internal Energy

Internal energy is characterized as the energy associated with the microscopic form of energy present in a system. It is mainly a result of the interactions between the adsorbent and the adsorbate. The variation in this energy is estimated using the following formula [43]:

$$E_{\text{int}} = -\frac{\partial \text{Ln}Z_{\text{gc}}}{\partial \beta} + \frac{\mu}{\beta} \left(\frac{\partial \text{Ln}Z_{\text{gc}}}{\partial \mu} \right) \quad (10)$$

where Z_{gc} is the total grand canonical partition function [25], μ is the chemical potential of the receptor sites [25], β is defined as $1/k_{\text{B}}T$, T is the absolute temperature, and k_{B} is the Boltzmann constant.

Figure 6 represents the variation in internal energy versus the concentration for the two tested systems. According to this figure, it is apparent that all the internal energy values are negative, confirming that the adsorption phenomenon is spontaneous. Consequently, these systems release energy during this process. Comparing the two adsorption systems, it is clear that the internal energy values of the MNIP adsorbents are higher than those of the MMIP adsorbents. This can be explained by the fact that MNIPs are synthesized through a molecular imprinting process, where the polymer is formed around a template molecule. This process may introduce additional energy due to the interactions between the polymer matrix and the template molecule during synthesis, resulting in higher internal energy in the resulting adsorbent [30,31]. Consequently, the MNIP sample requires more energy to remove the dexamethasone and hydrocortisone, confirming that MMIPs are more stable. This stability makes MMIPs suitable for the selective separation and enrichment of hydrocortisone and dexamethasone at low concentration levels in cosmetic samples.

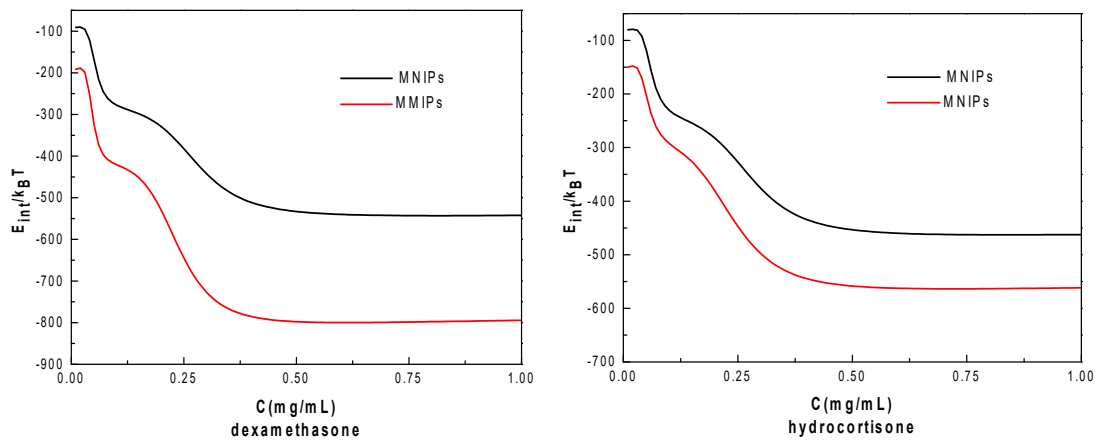


Figure 6. Evolution of internal energy versus hydrocortisone and dexamethasone concentration.

7.2. Gibbs Free Energy

This thermodynamic function defines the spontaneity of a system. It is determined using the following formula [43]:

$$G_a = \mu Q_a \quad (11)$$

where, μ is the chemical potential of the receptor sites and Q_a is the adsorption amount.

According to Figure 7, which depicts variation in the Gibbs energy as a function of concentration, we notice that the totality of the Gibbs energy values is less than zero, confirming the spontaneity of the adsorption phenomenon. Moreover, we note from this figure that when dexamethasone and hydrocortisone concentrations are low, adsorption is more favorable while at saturation. However, for elevated concentrations, the G_a of the two adsorption systems reach stable values despite these concentration increases. In addition, we observe that the Gibbs free energy values of the dual-template MMIPs towards the dexamethasone and hydrocortisone templates are significantly lower than those of the dual-template MNIPs. This difference can be attributed to the molecular imprinting process of the MMIPs, which ensures a tailored fit for the target molecules, and thus stronger and more selective binding compared with the MNIPs. This heightened specificity reduces the overall Gibbs free energy required for the interactions between the MMIPs and the template molecules, making the process more thermodynamically favorable. Consequently, the dual-template MMIPs exhibit lower Gibbs free energy values, indicating more stable and efficient interactions with dexamethasone and hydrocortisone compared with their MNIP counterparts.

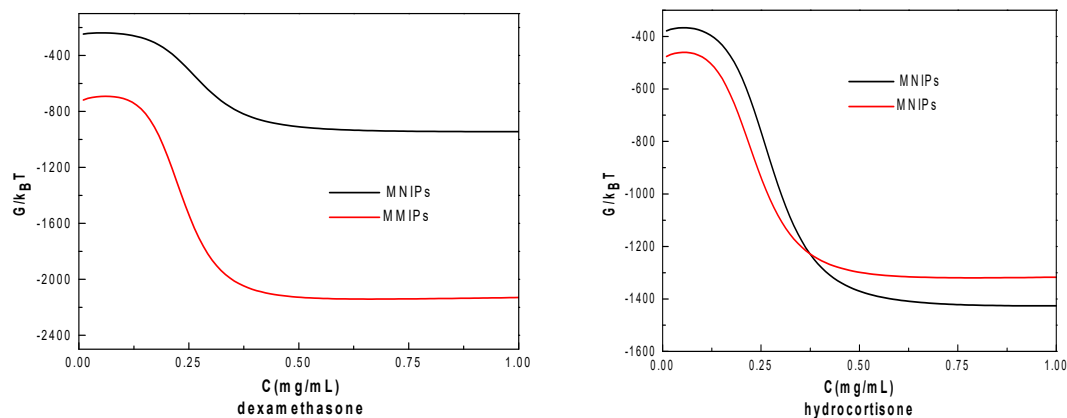


Figure 7. Evolution of Gibbs free energy versus hydrocortisone and dexamethasone concentration.

8. Conclusions

The adsorption of dexamethasone and hydrocortisone on dual-template MNIPs and MMIPs was theoretically analyzed. This technology has been applied successfully in the extraction of dexamethasone and hydrocortisone from cosmetic samples. A statistical multilayer model was applied to interpret various adsorption operating scenarios for cosmetic products using molecularly imprinted polymers. Statistical theory-based adjustments indicated that dexamethasone and hydrocortisone adsorption was affected through the creation of approximately two or three adsorbate layers. Moreover, it was theoretically shown that all cosmetic products were adsorbed via a non-parallel orientation onto the MMIP/MNIP surfaces. The adsorption of the tested samples was an exothermic physisorption process.

Author Contributions: F.A.: Formal analysis, Data curation; N.B.: Data curation, Validation; A.C.: Investigation Methodology; H.A.A.: Formal analysis, Data curation; A.B.L.: Supervision, Validation. All authors have read and agreed to the published version of the manuscript.

Funding: The authors extend their appreciation to the Deputyship for Research and Innovation, Ministry of Education in Saudi Arabia for funding this research work through the project number RI-44-0154.

Data Availability Statement: Data is contained within the article.

Conflicts of Interest: The authors declare no conflicts of interest.

References

1. Bornhövd, E.; Burgdorf, W.H.; Wollenberg, A. Macrolactam immunomodulators for topical treatment of inflammatory skin diseases. *J. Am. Acad. Dermatol.* **2001**, *45*, 736–743. [[CrossRef](#)]
2. Boumpas, D.T.; Chrousos, G.P.; Wilder, R.L.; Cupps, T.R.; Balow, J.E. Glucocorticoid therapy for immune-mediated diseases: Basic and clinical correlates. *Ann. Intern. Med.* **1993**, *119*, 1198–1208. [[CrossRef](#)]
3. Schäfer-Korting, M.; Mehnert, W.; Korting, H.C. Lipid nanoparticles for improved topical application of drugs for skin diseases. *Adv. Drug Deliv. Rev.* **2007**, *59*, 427–443. [[CrossRef](#)]
4. Rosso, J.D.; Friedlander, S.F. Corticosteroids: Options in the era of steroid-sparing therapy. *J. Am. Acad. Dermatol.* **2005**, *53*, S50–S58. [[CrossRef](#)]
5. Ference, J.D.; Last, A.R. Choosing topical corticosteroids. *Am. Fam. Physician* **2009**, *79*, 135–140. [[PubMed](#)]
6. Roozbahani, M.; Kharazih, M.; Emadi, R. pH sensitive dexamethasone encapsulated laponite nanoplatelets: Release mechanism and cytotoxicity. *Int. J. Pharm.* **2017**, *518*, 312–319. [[CrossRef](#)] [[PubMed](#)]
7. Katzung, B.G.; Masters, S.B.; Trevor, A.J. *Basic & Clinical Pharmacology: A Lange Medical Book*; McGraw-Hill Medical: New York, NY, USA, 2012.
8. Geraci, A.C.; Crane, J.S.; Cunha, B.A. Topical steroids; dosing forms and general considerations. *Hosp. Pharm.* **1991**, *26*, 699–719.
9. Santoni, O. *EU Cosmetics Regulation, Workshop on Natural Cosmetics*; University of Bangor: Bangor, UK, 2015; p. 2.
10. Kang, M.Q.; Sun, S.H.; Li, N.; Zhang, D.H.; Chen, M.Y.; Zhang, H.Q. Extraction and determination of hormones in cosmetics by homogeneous ionic liquid microextraction high-performance liquid chromatography. *J. Sep. Sci.* **2012**, *35*, 2032–2039. [[CrossRef](#)] [[PubMed](#)]
11. Shao, B.; Cui, X.; Yang, Y.; Zhang, J.; Wu, Y. Validation of a solid-phase extraction and ultra-performance liquid chromatographic tandem mass spectrometric method for the detection of 16 glucocorticoids in pig tissues. *J. AOAC Int.* **2009**, *92*, 604–611. [[CrossRef](#)] [[PubMed](#)]
12. Tong, S.; Liu, Q.; Li, Y.; Zhou, W.; Jia, Q.; Duan, T. Preparation of porous polymer monolithic column incorporated with graphene nanosheets for solid phase microextraction and enrichment of glucocorticoids. *J. Chromatogr. A* **2012**, *1253*, 22–31. [[CrossRef](#)]
13. Frerichs, V.A.; Tornatore, K.M. Determination of the glucocorticoids prednisone, prednisolone, dexamethasone, and cortisol in human serum using liquid chromatography coupled to tandem mass spectrometry. *J. Chromatogr. B* **2004**, *802*, 329–338. [[CrossRef](#)] [[PubMed](#)]
14. Luo, Y.; Uboh, C.; Soma, L.; Guan, F.; Rudy, J.; Tsang, D. Simultaneous analysis of twenty-one glucocorticoids in equine plasma by liquid chromatography/tandem mass spectrometry. *Rapid Commun. Mass Spectrom.* **2005**, *19*, 1245–1256. [[CrossRef](#)]
15. Mazzarino, M.; de la Torre, X.; Botrè, F. A screening method for the simultaneous detection of glucocorticoids, diuretics, stimulants, anti-oestrogens, beta-adrenergic drugs and anabolic steroids in human urine by LC-ESI-MS/MS. *Anal. Bioanal. Chem.* **2008**, *392*, 681–698. [[CrossRef](#)]
16. Li, X.; Li, M.; Li, J.; Lei, F.; Su, X.; Liu, M.; Li, P.; Tan, X. Synthesis and characterization of molecularly imprinted polymers with modified rosin as a cross-linker and selective SPE-HPLC detection of basic orange II in foods. *Anal. Methods* **2014**, *6*, 6397–6406. [[CrossRef](#)]

17. Su, X.; Li, X.; Li, J.; Liu, M.; Lei, F.; Tan, X.; Li, P.; Luo, W. Synthesis and characterization of core-shell magnetic molecularly imprinted polymers for solid-phase extraction and determination of Rhodamine B in food. *Food Chem.* **2015**, *171*, 292–297. [[CrossRef](#)]
18. Wei, S.; Li, J.; Liu, Y.; Ma, J. Development of magnetic molecularly imprinted polymers with double templates for the rapid and selective determination of amphenicol antibiotics in water, blood, and egg samples. *J. Chromatogr. A* **2016**, *1473*, 19–27. [[CrossRef](#)] [[PubMed](#)]
19. Liu, M.; Li, X.Y.; Li, J.J.; Su, X.M.; Wu, Z.Y.; Li, P.F.; Lei, F.H.; Tan, X.C.; Shi, Z.W. Synthesis of magnetic molecularly imprinted polymers for the selective separation and determination of metronidazole in cosmetic samples. *Anal. Bioanal. Chem.* **2015**, *407*, 3875–3880. [[CrossRef](#)]
20. Jing, T.; Wang, Y.; Dai, Q.; Xia, H.; Niu, J.; Hao, Q.; Mei, S.; Zhou, Y. Preparation of mixed-templates molecularly imprinted polymers and investigation of the recognition ability for tetracycline antibiotics. *Biosens. Bioelectron.* **2010**, *25*, 2218–2224. [[CrossRef](#)]
21. Liu, M.; Li, X.; Li, J.; Wu, Z.; Wang, F.; Liu, L.; Tan, X.; Lei, F. Selective separation and determination of glucocorticoids in cosmetics using dual-template magnetic molecularly imprinted polymers and HPLC. *J. Colloid Interface Sci.* **2017**, *504*, 124–133. [[CrossRef](#)] [[PubMed](#)]
22. Ben Lamine, A.; Bouazra, Y. Application of statistical thermodynamics to the olfaction mechanism. *J. Chem. Senses* **1997**, *22*, 67–75. [[CrossRef](#)] [[PubMed](#)]
23. Landin-Sandoval, V.J.; Mendoza-Castillo, D.I.; Seliem, M.K.; Mobarak, M.; Villanueva-Mejia, F.; Bonilla-Petriciolet, A.; Navarro-Santos, P.; Reynel-Ávila, H.E. Physicochemical analysis of multilayer adsorption mechanism of anionic dyes on lignocellulosic biomasses via statistical physics and density functional theory. *J. Mol. Liq.* **2021**, *322*, 114511. [[CrossRef](#)]
24. Priyanka, M.; Saravanakumar, M.P. New insights on aging mechanism of microplastics using PARAFAC analysis: Impact on 4-nitrophenol removal via Statistical Physics Interpretation. *Sci. Total Environ.* **2022**, *807*, 150819. [[CrossRef](#)]
25. Idrees, F.; Sibtain, F.; Junaid Dar, M.; Hassan Shah, F.; Alam, M.; Hussain, I.; Kim, S.J.; Idrees, J.; Khan, S.A.; Salman, S. Copper biosorption over green silver nanocomposite using artificial intelligence and statistical physics formalism. *J. Clean. Prod.* **2022**, *374*, 133991. [[CrossRef](#)]
26. Li, Z.; Sellaoui, L.; Franco, D.; Netto, M.S.; Georgin, J.; Dotto, G.L.; Bajahzar, A.; Belmabrouk, H.; Bonilla-Petriciolet, A.; Li, Q. Adsorption of hazardous dyes on functionalized multiwalled carbon nanotubes in single and binary systems: Experimental study and physicochemical interpretation of the adsorption mechanism. *Chem. Eng. J.* **2020**, *389*, 124467. [[CrossRef](#)]
27. Hua, P.; Sellaoui, L.; Franco, D.; Netto, M.S.; Dotto, G.L.; Bajahzar, A.; Belmabrouk, H.; Bonilla Petriciolet, A.; Li, Z. Adsorption of acid green and procion red on a magnetic geopolymer based adsorbent: Experiments, characterization and theoretical treatment. *Chem. Eng. J.* **2020**, *383*, 123113. [[CrossRef](#)]
28. Xue, H.; Gao, X.; Seliem, M.K.; Mobarak, M.; Dong, R.; Wang, X.; Fu, K.; Li, Q.; Li, Z. Efficient adsorption of anionic azo dyes on porous heterostructured MXene/biomass activated carbon composites: Experiments, characterization, and theoretical analysis via advanced statistical physics models. *Chem. Eng. J.* **2023**, *451*, 138735. [[CrossRef](#)]
29. Long, L.; Li, L.; Cheng, G.; Wei, S.; Wang, Y.; Huang, Q.; Wu, W.; Liu, X.; Chen, G. Study of the Preparation and Properties of Chrysin Binary Functional Monomer Molecularly Imprinted Polymers. *Polymers* **2022**, *14*, 2771.
30. Takeuchia, T.; Haginaka, J. Separation and sensing based on molecular recognition using molecularly imprinted polymers. *J. Chromatogr. B Biomed. Sci. Appl.* **1999**, *728*, 1–20. [[CrossRef](#)] [[PubMed](#)]
31. Nishino, H.; Huang, C.S.; Shea, K.J. Selective protein capture by epitome imprinting. *Angew. Chem. Int. Ed. Engl.* **2006**, *45*, 2392–2396. [[CrossRef](#)]
32. Chen, L.X.; Wang, X.Y.; Lu, W.H.; Wu, X.Q.; Li, J.H. Molecular imprinting: Perspectives and applications. *Chem. Soc. Rev.* **2016**, *45*, 2137–2211. [[CrossRef](#)]
33. Bel Haj Mohamed, N.; Bouzidi, M.; Ouni, S.; Alshammari, A.S.; Khan, Z.R.; Gandouzi, M.; Mohamed, M.; Chaaben, N.; Bonilla-Petriciolet, A.; Haouari, M. Statistical physics analysis of adsorption isotherms and photocatalysis activity of MPA coated CuInS₂/ZnS nanocrystals for the removal of methyl blue from wastewaters. *Inorg. Chem. Commun.* **2022**, *144*, 109933. [[CrossRef](#)]
34. Pang, X.; Sellaoui, L.; Franco, D.; Netto, M.S.; Georgin, J.; Dotto, G.L.; Abu Shayeb, M.K.; Belmabrouk, H.; Bonilla-Petriciolet, A.; Li, Z. Preparation and characterization of a novel mountain soursop seeds powder adsorbent and its application for the removal of crystal violet and methylene blue from aqueous solutions. *Chem. Eng. J.* **2020**, *391*, 123617. [[CrossRef](#)]
35. Zheng, P.L.; Zhang, B.L.; Luo, Z.M.; Du, W.; Guo, P.Q.; Zhou, Y.L.; Chang, R.M.; Chang, C.H.; Fu, Q. Facile preparation of polydopamine-coated imprinted polymers on the surface of SiO₂ for estrone capture in milk samples. *J. Sep. Sci.* **2016**, *41*, 2585–2594. [[CrossRef](#)]
36. Wang, H.; Li, Z.; Yahyaoui, S.; Hanafy, H.; Seliem, M.K.; Bonilla-Petriciolet, A.; Dotto, G.L.; Sellaoui, L.; Li, Q. Effective adsorption of dyes on an activated carbon prepared from carboxy- methyl cellulose: Experiments, characterization and advanced modeling. *Chem. Eng. J.* **2021**, *417*, 128116. [[CrossRef](#)]
37. Zhang, L.; Sellaoui, L.; Franco, D.; Dotto, G.L.; Bajahzar, A.; Belmabrouk, H.; Bonilla-Petriciolet, A.; Oliveira, M.L.S.; Li, Z. Adsorption of dyes brilliant blue, sunset yellow and tartrazine from aqueous solution on chitosan: Analytical interpretation via multilayer statistical physics model. *Chem. Eng. J.* **2020**, *382*, 122952. [[CrossRef](#)]

38. Ramadan, H.S.; Ali, R.A.M.; Mobarak, M.; Badawi, M.; Selim, A.Q.; Mohamed, E.A.; Bonilla-Petriciolet, A.; Seliem, M.K. One-step fabrication of a new outstanding rutile TiO₂ nanoparticles/anthracite adsorbent: Modeling and physicochemical interpretations for malachite green removal. *Chem. Eng. J.* **2021**, *426*, 131890. [[CrossRef](#)]
39. Bouzid, M.; Bouaziz, N.; Torkia, Y.B.; Lamine, A.B. Statistical physics modeling of ethanol adsorption onto the phenol resin based adsorbents: Stereographic, energetic and thermodynamic investigations. *J. Molec. Liq.* **2019**, *283*, 674–687. [[CrossRef](#)]
40. Ben Torkia, Y.; Khalfaoui, M.; Ben Lamine, A. On the use of the Hill model as a local isotherm in the interpretation of the behaviour of the adsorption energy distributions. *IOSR J. Appl.* **2014**, *63*, 62–73. [[CrossRef](#)]
41. Lin, C.H.; Lee, S.C.; Chen, Y.F. Strong room-temperature photoluminescence of hydrogenated amorphous silicon oxide and its correlation to porous silicon. *Appl. Phys. Lett.* **2014**, *63*, 62–73. [[CrossRef](#)]
42. Kumar, K.V.; de Castro, M.M.; Martinez-Escandell, M.; Molina-Sabio, M.; Silvestre-Albero, J.; Rodriguez-Reinoso, F. A continuous site energy distribution function from Redlich–Peterson isotherm for adsorption on heterogeneous surfaces. *Chem. Phys. Lett.* **2010**, *492*, 187–192. [[CrossRef](#)]
43. Diu, B.; Guthmann, C.; Lederer, D.; Roulet, B. Macroscopic motion of a totally isolated system in statistical equilibrium. *Am. J. Phys.* **1990**, *58*, 974–978. [[CrossRef](#)]

Disclaimer/Publisher’s Note: The statements, opinions and data contained in all publications are solely those of the individual author(s) and contributor(s) and not of MDPI and/or the editor(s). MDPI and/or the editor(s) disclaim responsibility for any injury to people or property resulting from any ideas, methods, instructions or products referred to in the content.